Neurobiology of Aging 126 (2023) 14–24

Contents lists available at ScienceDirect

Neurobiology of Aging

journal homepage: www.elsevier.com/locate/neuaging.org

Sex differences in brain metabolic connectivity architecture in probable dementia with Lewy bodies

Silvia Paola Caminiti[a,b], Cecilia Boccalini[a,b,c], Nicolas Nicastro[d,e], Valentina Garibotto[c,f,g], Daniela Perani[a,b,*], The Alzheimer's Disease Neuroimaging Initiative[#]

[a] School of Psychology, Vita-Salute San Raffaele University, Milan, Italy
[b] Division of Neuroscience, IRCCS San Raffaele Scientific Institute, Milan, Italy
[c] Laboratory of Neuroimaging and Innovative Molecular Tracers (NIMTlab), Geneva University Neurocenter and Faculty of Medicine, University of Geneva, Geneva, Switzerland
[d] Division of Neurorehabilitation, Department of Clinical Neurosciences, Geneva University Hospitals, Geneva, Switzerland
[e] Faculty of Medicine, University of Geneva, Geneva, Switzerland
[f] Division of Nuclear Medicine and Molecular Imaging, Geneva University Hospitals, Geneva, Switzerland
[g] Center for Biomedical Imaging (CIBM), Geneva, Switzerland

ARTICLE INFO

Article history:
Received 8 November 2022
Revised 23 January 2023
Accepted 10 February 2023
Available online 17 February 2023

Keywords:
Sex
Neurodegeneration
Alpha-synuclein
Vulnerability
Brain Hypometabolism

ABSTRACT

We investigated how sex modulates metabolic connectivity alterations in probable dementia with Lewy bodies (pDLB).

We included 131 pDLB patients (males/females: 58/73) and similarly aged healthy controls (HC) (male/female: 59/75) with available (18)F-fluorodeoxyglucose positron emission tomography (FDG-PET) scans. We assessed (1) sex differences in the whole-brain connectivity, identifying pathological hubs, (2) connectivity alterations in functional pathways of the neurotransmitter systems, (3) Resting State Networks (RSNs) integrity.

Both $pDLB_M$ (males) and $pDLB_F$ (females) shared dysfunctional hubs in the insula, Rolandic operculum, and inferior parietal lobule, but the $pDLB_M$ group showed more severe and diffuse whole-brain connectivity alterations. Neurotransmitters connectivity analysis revealed common alterations in dopaminergic and noradrenergic pathways. Sex differences emerged particularly in the Ch4-perisylvian division, with $pDLB_M$ showing more severe alterations than $pDLB_F$. The RSNs analysis showed no sex differences, with decreased connectivity strength in the primary visual, posterior default mode, and attention networks in both groups.

Extensive connectivity changes characterize both males and females in the dementia stage, with a major vulnerability of cholinergic neurotransmitter systems in males, possibly contributing to the observed different clinical phenotypes.

1. Introduction

Several sex differences in brain structure and function exist in healthy participants (Ingalhalikar et al., 2014; Ruigrok et al., 2014) and neurological conditions (Ballmaier et al., 2004; Boccalini et al., 2022; Malpetti et al., 2017). These seem to modulate the manifestation and progression of clinical phenotypes.

Sex studies in dementia traditionally report a higher proportion of women with Alzheimer's disease (AD), and men with Parkinson's disease (PD) with a 2:1 male/female ratio in the latter (Caslake et al., 2013; Podcasy & Epperson, 2022). Therefore, sex seems a valuable parameter to be considered when designing predictive models for disease prevention, diagnosis, and possibly treatment response (Ferretti et al., 2018). Moreover, the study of sex differences in neurodegenerative conditions may help us understand how and why male and female brains differ in their predisposition for risk or resilience (Ruigrok et al., 2014).

* Corresponding author at: Division of Neuroscience, San Raffaele Scientific Institute Nuclear Medicine Unit, Vita-Salute San Raffaele University, San Raffaele Hospital, Via Olgettina 60, Milan 20132, Italy Tel.: (+39) 02.2643.2224.
E-mail address: perani.daniela@hsr.it (D. Perani).

[#] Data used in the preparation of this article were obtained from the Alzheimer's Disease Neuroimaging Initiative (ADNI) database (adni.loni.usc.edu). The investigators of the ADNI contributed to the design and implementation of the ADNI and/or provided data, but they did not participate in the analysis or writing of this report. A complete list of the ADNI investigators can be found at http://adni.loni.usc.edu/wpcontent/uploads/how_to_apply/ADNI_Acknowledgement_List.pdf.

0197-4580/$ – see front matter © 2023 Elsevier Inc. All rights reserved.
https://doi.org/10.1016/j.neurobiolaging.2023.02.004

Dementia with Lewy bodies (DLB) is the second most common neurodegenerative dementia after AD. The DLB core symptoms often manifest in different combinations at diagnosis or during the disease course (Abdelnour et al., 2022), and sex might play a role in this heterogeneity (Bayram et al., 2021; Dugger et al., 2012). A diagnosis of DLB is more likely to be done in males than females (Mouton et al., 2018). DLB males express more neocortical "diffuse" Lewy bodies (LB) at post mortem pathology than females (women = 6.4%; men = 9.5%; $p < 0.05$) (Barnes et al., 2019), and a balanced male/female ratio for mixed AD/LB pathology (Bayram et al., 2022; Nelson et al., 2010). Women were more likely to have AD with advanced TDP-43 or Hippocampal sclerosis than men (women = 27.0%; men = 19.9%; $p < 0.01$) (Barnes et al., 2019). When controlling for age, women showed less CSF *α-synuclein* and more *β-amyloid 1–42* pathology than men (Van de Beek et al., 2020). There is evidence that a significant proportion of women are clinically diagnosed with AD despite underlying LB pathology (Bayram et al., 2021). LB pathology may not have the same clinical impact on women as on men.

Male brain is characterized by larger within-hemisphere connectivity, with a high level of modularity, whereas female brain shows greater interhemispheric connectivity and greater cross-hemispheric participation. The structural connectivity differences are also supported by behavioral data, with females outperforming males on attention, word and face memory, and social cognition tests, while males performed better on spatial processing and (sensory) motor speed (Gur et al., 2012; Ingalhalikar et al., 2014). Neurodegeneration acts on molecular pathways, and local circuits in specific brain regions, producing reconfigurations and loss of functions in higher-order neural networks (Carli et al., 2021). As for development, sex may differentially affect the trajectories of connectome dysfunction in neurodegeneration.

Previous studies using different neuroimaging modalities show widespread abnormalities within and across brain networks in DLB (recently reviewed by [Habich et al., 2022]). In particular, FDG-PET revealed substantial and widespread impairment of brain metabolic connectivity in DLB (Caminiti et al., 2017; G. Carli et al., 2020; Sala et al., 2019), with alterations in large-scale resting-state networks also significantly and specifically associated with the core DLB clinical symptoms (Sala et al., 2019).

The neurotransmitter changes reported in DLB mostly include a degeneration of the dopaminergic, cholinergic and noradrenergic systems (Caminiti & Carli, 2023; Francis & Perry, 2007). A dysregulated noradrenergic (NA) innervation, possibly related to α-synuclein pathology, is emerging as pathological mechanisms associated with early rapid eye movement sleep behaviour disorder (RBD), neuropsychiatric symptoms, and autonomic deficits, characterizing DLB (Pfeiffer, 2016). We previously found alterations in the DLB brain metabolic networks connectivity as a result of dysfunction in DA, NA and Ch neurotransmission systems (Carli et al., 2020). No study has hitherto investigated sex-related brain connectivity alterations in DLB, which, instead, have been assessed in PD (Boccalini et al., 2022, 2020) and AD (Malpetti et al., 2017) conditions. Notably, studies in PD (which shares with DLB the *α-synuclein* protein pathology and dopaminergic deficits), have shown a more prevalent impairment of dorsal dopaminergic network in males compared to females (Boccalini et al., 2020).

In the current study, we investigated how sex can modulate brain metabolism and metabolic connectivity of whole-brain networks in DLB. We also tested a comprehensive model focusing on the DA, NA, and Ch-divisions systems to explore connectivity reconfiguration in major biochemical circuits for DLB. We also evaluated connectivity changes in the resting-state networks (RSNs) that are linked to core processes of human cognition (van Den Heuvel & Pol, 2010) and found to be vulnerable in DLB (Sala et al., 2019).

2. Materials and methods

2.1. Participants

One hundred and thirty-one DLB patients (mean age in years ± standard deviation [SD]: 72 ± 7.8; sex [F/M]: 58/73) fulfilling the latest consensus criteria for diagnosis of probable DLB (pDLB) were retrospectively included from the clinical and imaging database of San Raffaele Hospital (Milan, Italy) and Geneva University Hospitals (Switzerland). Clinical diagnosis of pDLB was made in the presence of at least 2 core symptoms (i.e., cognitive fluctuations, visual hallucination (VH), or parkinsonism), or one core symptom plus at least one suggestive feature (i.e., RBD, severe neuroleptic sensitivity, or low dopamine transporter uptake at SPECT) (McKeith et al., 2017). All patients underwent magnetic resonance imaging or computer tomography to exclude an underlying pathology (e.g., cerebrovascular disease).

Patients showing any neurological and psychiatric comorbidities were excluded from the study.

The 2 clinical groups ($pDLB_M$ and $pDLB_F$) were compared through a one-way analysis of variance for continuous variables and Pearson's χ^2 test for frequencies (Table 1). SPSS 21.0 software for Windows (SPSS, Chicago, IL, United States) was used to perform statistical analyses.

We selected FDG-PET scans of 67 healthy controls (HC) from the control imaging database of the Nuclear Medicine Unit, San Raffaele Hospital, Milan. To obtain an equal sample size with the 2 pDLB groups and to avoid inter-scanner variability, we added 67 FDG-PET images from the ADNI database (adni.loni.usc.edu). ADNI is a multi-site US public-private partnership launched in 2003 and led by Principal Investigator Michael W. Weiner, MD. The primary goal of ADNI has been to test whether biomarkers, clinical and neuropsychological assessments can be combined to predict conversion to Alzheimer's disease (AD). For up-to-date information, see https://adni.loni.usc.edu.

The final group of 134 HC comprised 75 males and 59 females with a similar age to DLB subjects (mean age F: 73 ± 4, t = -0.65 $p = 0.52$; M: 70 ± 6, t = 1.88 $p = 0.07$).

Written informed consent was obtained from participants. The study was approved by San Raffaele Hospital of Milan (Study Protocol FDG PET Metabolic Patterns version n°2) and University of Geneva Ethic Committees (Study Protocol NO 2022-01520, Geneva, Switzerland) and conducted in compliance with the Declaration of Helsinki for the protection of human participants.

2.2. FDG-PET image acquisition and reconstruction

The FDG-PET acquisitions (100 pDLB patients and 67 HC) performed at the Nuclear Medicine Unit, San Raffaele Hospital were acquired using the same Discovery STE PET (3.27-mm thickness; in-plane FWHM 5.55-mm) manufactured by GE Healthcare; 31 FDG-PET scans were performed at the nuclear medicine and molecular imaging division at Geneva University Hospitals with Biograph128 mCT, Biograph128 Vision 600 Edge, Biograph40 mCT, or Biograph64 TruePoint PET scanners (Siemens Medical Solutions, USA). FDG-PET images belonging to ADNI subjects were obtained using ECAT HR+, General Electric Discovery LS, General Electric Discovery ST, General Electric Discovery STE, Siemens/ECAT HRRT, Siemens Biograph Hi-Rez, Philips Gemini TF, Siemens mCT and ECAT Biograph.

The acquisitions conformed to the European Association of Nuclear Medicine guidelines. Static emission images were acquired 30 to 45-minute after injecting 185–250 MBq of [18F]FDG via an intravenous cannula. This postinjection time interval allows obtaining an equal distribution of the tracer across the entire brain, with

Table 1
Demographic and clinical features at entry

	pDLB	$pDLB_F$	$pDLB_M$	Sign.
N	**131**	**58**	**73**	
Age (mean±SD)	72.34 ±7.8	72.43±8	72.27±7.7	0.91
Education[a]	10.14±4.32	9.31±3.58	10.63±4.7	0.06
Disease duration (mean±SD)	2.26±1.8	2.47±2.13	2.12±1.5	0.332
MMSE (mean±SD)	18.9±5.2	18.6±5.2	19.05±5.3	0.714
Parkinsonism %	88%	89%	88%	0.884
Visual hallucinations %	62%	52%	67%	0.183
Cognitive fluctuations %	46%	41%	49%	0.490
RBD %	40.3%	31%	46%	0.216

Key: pDLB, probable dementia with Lewy bodies; RBD, rapid eye movement sleep behaviour disorder; SD, Standard Deviation.
[a] data available in 96 DLB patients.

negligible blood flow-dependent differences, thus achieving an optimal signal-to-noise ratio. The duration of scan acquisition was 15/20 minute.

The 67 steady-state emission images obtained from the ADNI dataset were acquired 30 minute after injecting approximately 185MBq of [18F]FDG, with a 30-minute scan acquisition duration. After realignment to correct for interframe motion, only the last three 5-minute frames were retrieved from the ADNI database and combined to obtain a single 15-minute static image, to increase uniformity across acquisition procedures. Uniform reconstruction protocols were applied, for example, the ordered subset expectation maximization algorithm and CT attenuation correction procedures. The San Raffaele Hospital and ADNI HC datasets were previously compared and validated by our group (Caminiti et al., 2021).

2.3. Preprocessing

A rigorous quality control process was performed to check potential artifacts (e.g., acquisition issues, excessive patient motion) and issues related to technical characteristics, such as the use of compatible reconstruction algorithms. Then, FDG-PET images of patients and controls were normalized to the optimized FDG-PET template (Della Rosa et al., 2014), using SPM12 (https://www.fil.ion.ucl.ac.uk/spm/). They were then scaled to the global mean of the activity within the brain and finally smoothed with an isotropic 3D Gaussian kernel (8 mm Full Width Half Maximum), accordingly to the validated pipeline proposed for our single-subject SPM-based analysis (Perani et al., 2014). This validated SPM-based procedure has been demonstrated to provide reliable results regardless of the scanners used for image acquisition (Presotto et al., 2017).

2.4. Group analysis

A voxel-wise group analysis, employing a 2-sample t-test on SPM, was applied to compare the 2 pDLB groups with the sex-matched HC groups ($pDLB_M < HC_M$; $pDLB_F < HC_F$) thus obtaining the common hypometabolism patterns for $pDLB_M$ and $pDLB_F$. The statistical threshold was set at $p = 0.05$, family-wise error (FWE)-corrected for multiple comparisons. Only clusters containing more than 100 voxels were deemed to be significant.

Following the same approach, we directly compared the 2 pDLB groups ($pDLB_M < pDLB_F$; $pDLB_F < pDLB_M$). Due to the high level of brain metabolic similarity between the 2 clinical groups, the statistical threshold was set at $p = 0.001$, without applying a correction for multiple comparisons.

All the SPM group comparisons were performed considering age as a variable of no interest.

In addition, a linear regression analysis was applied in SPM12 to assess the voxel-level correlations between age and whoile brain glucose metabolism, considering the smoothed and warped images of the HC males and females, separately.

2.5. Metabolic connectivity–whole-brain and neurotransmitters networks

Brain metabolic connectivity analysis was applied to investigate the molecular architecture of the whole-brain network and the major neurotransmission circuits, namely the dorsal and ventral dopaminergic, noradrenergic, and cholinergic pathways. The metabolic connectivity approach relies on the assumption that regions with similar metabolic demands are functionally associated (Horwitz et al., 1984).

The metabolic connectivity procedure consisted of the following steps: (1) selection of Regions of Interest (ROIs) for the networks' construction. We considered the whole-brain network by applying the Automated anatomical labeling (AAL) (Tzourio-Mazoyer et al., 2002) for cortical, subcortical, and cerebellar regions (95 × 95 ROIs). Neurotransmitter networks were created following Carli et al. (Carli et al., 2020) for the dorsal dopaminergic, noradrenergic, and cholinergic circuits, and Perani et al. (Perani et al., 2021) for the ventral dopaminergic circuit. To minimize the partial volume effect, only ROIs with a mean volume above 2 × FWHM of spatial resolution of our PET-CT system in all directions were considered for the analysis; (2) extraction of FDG uptake normalized by global brain uptake from each ROI; (3) creation of a subject-by-ROI matrix for each group ($pDLB_M$ - $pDLB_F$ - HC_M - HC_F); (4) assessment of linear correlation between nodes across subjects, obtaining an adjacency matrix for each group and the considered networks; (5) assessment of significant ($p<0.01$) changes in correlation coefficients - indexing alterations (loss and gain) in metabolic connectivity - between pDLB and HC groups for each network. The between-group comparison was performed by applying a z-test to the Fisher's transformed correlation coefficients; (6) extraction of the "altered connectivity" by counting the number of significant changes, obtained from the comparison between patients and HC; (7) comparison of the percentage of altered metabolic connections between male and female patients for each network through the $\chi 2$ test; (8) extraction of "pathological hub" defined as the ROIs with a percentage of altered connectivity one standard deviation above the total number of altered connections in the diagnostic group.

The analysis was run using MATLAB software (http://it.mathworks.com/products/matlab/) Mathworks Inc., Sherborn, Mass., USA).

2.6. Metabolic connectivity–resting-state networks

Voxel-wise seed-based interregional correlation analysis (IRCA) was applied to derive resting-state metabolic networks starting

from proper seed regions (Lee et al., 2008; Sala et al., 2019). We selected seed regions of individual large-scale networks previously determined by extensive and relevant literature (Jones et al., 2011; Karahanoğlu & Van an De Ville, 2015; Seeley et al., 2007; Shirer et al., 2012; Tomasi & Volkow, 2011). We selected the posterior cingulate cortex and precuneus for the posterior default mode network (pDMN); calcarine and lateral occipital cortex, respectively for the primary (PVN) and higher visual (HVN) networks; the inferior parietal lobule for the attention networks (ATN); the dorsolateral prefrontal cortex (DLPFC) for the executive network (EXN); the amygdala for the limbic network (LIN); the precentral gyrus for the motor network (MN). Seed ROIs were defined from functional resting-state networks atlas (Shirer et al., 2012) (findlab.stanford.edu/ functional_ROIs.html). Since not all seed ROIs were available in this atlas, we added a set of ROIs derived from other dedicated atlases: the inferior parietal lobule was derived from the Jülich histological atlas (Eickhoff et al., 2005); the DLPFC, derived from Sallet's Dorsal Frontal Parcellation Atlas (Sallet et al., 2013); the amygdala, derived from AAL atlas (Tzourio-Mazoyer et al., 2002).

For each network, the average seed uptake was set as a variable of interest in a multiple regression model in SPM12, entering age as a nuisance covariate, and testing for whole-brain voxel-wise correlations. Statistical significance at $p < 0.05$, FWE corrected for multiple comparisons, and minimum cluster extent set at cluster extent > 100 voxels, was considered as a reasonable trade-off between statistical robustness and sensitivity (Bennett et al., 2009).

2.6.1. Jaccard Similarity Coefficient analysis

The Jaccard Similarity Coefficient (JSC), a well-established and used metric for connectivity analysis (Jovicich et al., 2016; Karahanoğlu & Van De Ville, 2015; Sala et al., 2019), was applied to assess the concordance of connectivity alterations found in pDLB groups in the whole-brain and neurotransmitters' networks. The JSC was computed by considering the commonly altered connections between the 2 groups normalized to the total number of connections in the same groups. JSC was also applied to measure the voxel-by-voxel spatial similarity of RSNs between pDLB and HC groups and between $pDLB_M$ and $pDLB_F$. In this case, the JSC was calculated considering the number of voxels in the intersection between the considered RSN binary masks, normalized to the number of voxels extracted from the sum of the RSN binary masks. JSC ranges from 0, indicating no overlap across the 2 groups, to 1, indicating complete overlap.

3. Results

3.1. Group analysis

Brain hypometabolism pattern for both males and females corresponded to the prototypical DLB-like pattern, involving the bilateral medial and lateral occipital, temporoparietal, as well as dorsolateral prefrontal cortex (Fig. 1).

Direct statistical comparison between the 2 pDLB groups showed that $pDLB_M$ showed a more severe brain hypometabolism in the occipital, temporoparietal cortex, and cerebellum Crus I/II. Instead, $pDLB_F$ showed a more extended hypometabolism in the hippocampal structures, compared to $pDLB_M$ (Fig. 1).

In HC, we found statistically significant negative correlations between age and whole brain glucose metabolism in males and females. Namely, an extended reduction of brain metabolism in the medial prefrontal cortex, anterior and middle cingulate gyrus in males, limited to the anterior cingulate cortex in females (Supplementary Fig. 1).

3.2. Metabolic connectivity

Whole-brain network – Overall, a pattern of significant whole-brain reconfigurations, mostly involving connectivity losses, was found in the 2 clinical groups as compared to HC (Fig. 2A). The 2 groups shared 18% of altered connections according to the JSC analysis. The $pDLB_M$ group showed a significantly higher proportion of altered connectivity (20%) than the $pDLB_F$ (9.7%) ($\chi^2=3.92$, $p<0.05$). There were mostly connectivity losses in $pDLB_M$, involving temporal, insular, and cerebellar nodes, whereas female connectome featured patterns of increased connectivity; in particular, we found increased connectivity among the insula node and olfactory cortex, amygdala, hippocampus, thalamus, putamen and pallidum, and the olfactory node with the insula, temporal pole, and occipital cortex (Fig. 2A).

Hubs - In both groups, common pathological hubs were the bilateral angular gyrus and the Rolandic operculum, the left inferior parietal lobule, and the right insula (Fig. 2B). All these hubs significantly lost reciprocal connections as well as with a series of widespread cortical nodes (Fig. 2A). Then, we identified the nodes that resulted as pathological hubs only for males or females. The $pDLB_M$ showed selective pathological hubs in the inferior and right middle temporal gyrus, fusiform gyrus, left Rolandic operculum, left gyrus rectus, and right supramarginal gyrus. Instead, the $pDLB_F$ group showed selective pathological hubs in the superior and middle frontal cortex, left olfactory cortex, left insula, Heschl gyrus, right inferior parietal cortex, and precuneus (see Fig. 2B).

Dorsal DA network – The JSC analysis identified an overlap of 17% of connectivity alterations in the 2 DLB groups, with shared common striato-frontal connectivity alterations, specifically involving the dorsal putamen and the middle and superior frontal gyrus. There were also different connectivity patterns (Fig. 3). For instance, the dorsal caudate connectivity was affected in males, but not in females who, instead, showed disconnections among cortical nodes.

Ventral DA network – We found a similar connectivity pattern of alterations in the 2 groups, supported by a JSC, equal to 22%. However, the $pDLB_M$ group showed connectivity alterations in 20% of nodes versus the 7% found in the $pDLB_F$ group ($\chi^2=7.24$, $p<0.001$). In detail, both $pDLB_M$ and $pDLB_F$ showed a loss of connectivity between the right frontal cortex pars orbitalis and the left homologous region. We also found disconnections across the olfactory cortex, parahippocampal gyrus, and anterior cingulate cortex in the 2 pDLB groups (Fig. 3). Of note, the ventral striatum was disconnected from the orbitofrontal cortex only in males. Moreover, the $pDLB_F$ group showed a prevalent connectivity loss on the right side of the network, which in the $pDLB_M$ extended to the contralateral side (Fig. 3).

NA network – Overall, similar connectivity changes were found in the 2 groups, with a JSC equal to 25%, with a 16% and 12% connectivity alteration in $pDLB_M$ and $pDLB_F$, respectively ($\chi^2=0.6645$, $p=0.5$). We found common disconnections between the middle frontal cortex and the hypothalamus, amygdala, hippocampus, and precentral lobule. Furthermore, the precuneus was disconnected from the hypothalamus, amygdala, hippocampus, precentral, and postcentral lobule. Local disconnections between cerebellar nodes were also found in the 2 groups (Fig. 3).

Ch3 network – This network showed no difference in the 2 clinical groups as compared to sex-matched HC.

Ch4-Perisylvian Network - We found no overlap in network alterations between the 2 groups. The Ch4-Perisylvian division showed 31.5% connectivity alterations in the $pDLB_M$, which was significantly different from a 7.6% alteration found in the $pDLB_F$ group ($\chi^2=18$, $p<0.001$). The $pDLB_M$ was characterized by widespread loss of connectivity between the inferior frontal cor-

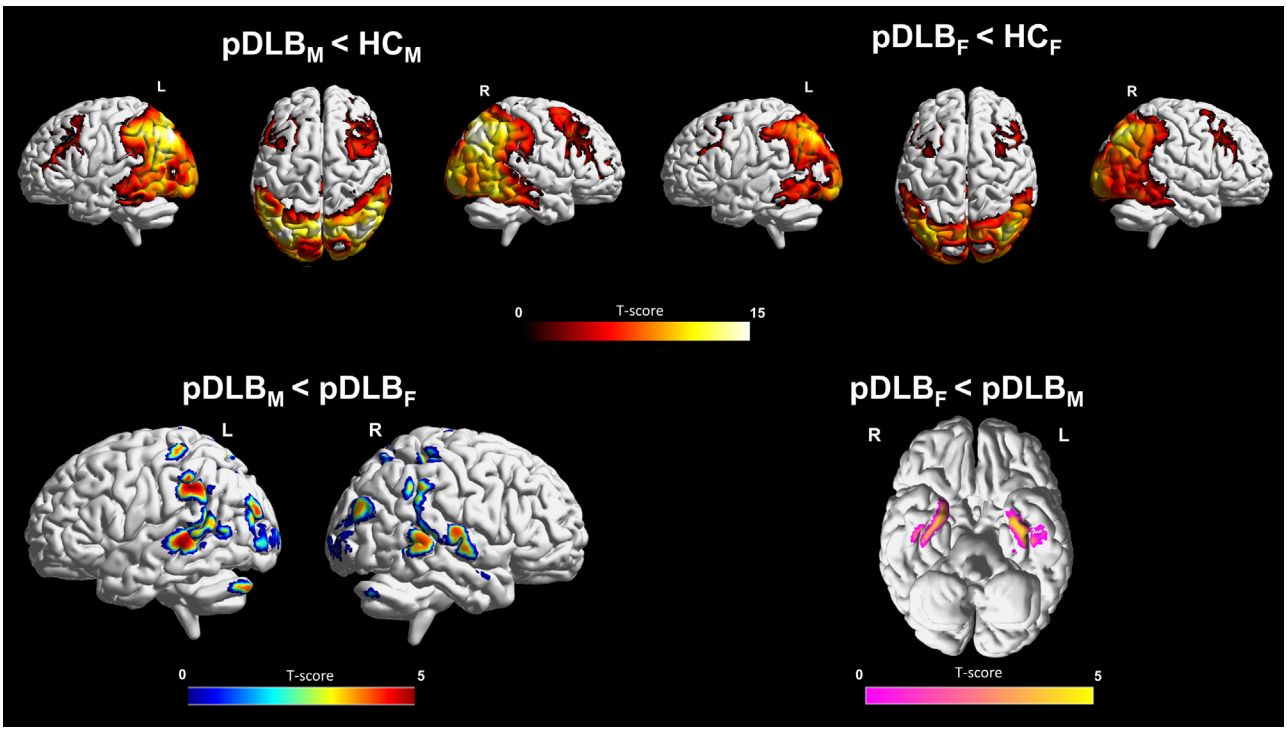

Fig. 1. Topographical distribution of brain hypometabolism. Top: FDG-PET SPM group comparisons between pDLB and controls. Yellow/red scale represents hypometabolism severity in pDLB compared to HC (pFWE < 0.05, k = 100). Bottom: FDG-PET SPM group comparisons of $pDLB_M$ and $pDLB_F$. Blue/red scale represents hypometabolism in $pDLB_M$ versus $pDLB_F$ ($p < 0.001$, uncorrected, k = 100); Pink/yellow scale represents hypometabolism in $pDLB_F$ versus $pDLB_M$ ($p < 0.001$, uncorrected, k = 100). 3D renderings were obtained from BrainNet Viewer toolbox (Xia et al., 2013). Abbreviations: F, females; HC, healthy controls L, left; M, males; pDLB, probable dementia with Lewy bodies;R, right. (For interpretation of the references to color in this figure legend, the reader is referred to the Web version of this article.)

tex nodes and the Rolandic operculum, Heshl gyrus, insula, and olfactory cortex. Instead, the $pDLB_F$ showed altered connectivity increases between the superior temporal pole and the Rolandic operculum, Heshl gyrus, insula, and olfactory cortex, without evidence of loss of connectivity.

Ch4-Median network – The 2 pDLB groups showed no overlap in the affected nodes (JSC = 0%). Specifically, the $pDLB_F$ group showed statistically significant altered connectivity only in 8% of nodes, with a loss of connections involving the superior frontal gyrus and anterior cingulate cortex, superior frontal gyrus pars orbitalis, and gyrus rectus. The $pDLB_M$ showed altered connectivity in 5% of nodes (χ^2=0.740, p=0.39), involving the middle, medial and superior frontal gyrus pars orbitalis, gyrus rectus, and anterior cingulate cortex (Fig. 3). Male connectivity alterations involved both increases and decreases, whereas only decreases were present in females.

Ch5-6 network – Both groups showed increased connectivity as compared to HC, without evidence of reduced connectivity. According to the JSC analysis, we found no overlap in connectivity alterations between $pDLB_M$ and $pDLB_F$, with different nodes involved in males and females: the connectivity of dorsal putamen and pallidum were affected in $pDLB_F$, whereas in $pDLB_M$ the dorsal caudate and ventral striatum (Fig. 3).

RSNs - Fig. 4 illustrates the connectivity changes for each large-scale network in the 2 pDLB groups. There was a good overlap (JSC $\geq$ 40%) between $pDLB_F$ and $pDLB_M$ in most networks, except for the limbic and motor ones. The highest levels of overlap between the 2 clinical groups were found in the primary visual, posterior default mode, and attention networks. In these RSNs, both groups showed decreases in the overall connectivity strength as compared to HC (JSC $\leq$ 25%). Instead, connectivity alterations were prominent in the executive, limbic, and higher visual networks for $pDLB_M$ than $pDLB_F$ group as compared to HC. In particular, the high visual network was the most altered network for males (JSC = 20%), but not for females (JSC = 36%).

4. Discussion

In the current study, we found commonalities and differences in a large cohort of pDLB patients stratified by sex, and characterized by similar age, global cognitive functioning, and disease duration at the time of FDG-PET exam. We applied metabolic connectivity approaches in a comprehensive whole brain and neural networks perspective to shed light on possible metabolic sex differences in pDLB.

In the current study, both male and female pDLB groups showed the prototypical DLB-like hypometabolism, involving the occipital, temporoparietal cortex, and dorsolateral prefrontal cortex (Caminiti et al., 2019). However, the direct comparison revealed a more severe hypometabolism in temporoparietal and occipital DLB signature regions in $pDLB_M$ than $pDLB_F$ patients (Fig. 1). Despite greater frontal and parietal volume loss in men than women have been reported in DLB contributing to cognitive dysfunction (Ballmaier et al., 2004), this is the first time that sex differences in brain hypometabolism are investigated in pDLB. The more severe brain posterior hypometabolism in men compared to women may be due to the more diffuse neocortical LB pathology found in $pDLB_M$ (Nelson et al., 2010), which is also considered the main determinant of occipital hypometabolism in DLB (Kasanuki et al., 2012). The latter was associated with worse global cognitive dysfunction, visuo-spatial, and visuo-perceptive deficits, and with a higher likelihood of developing visual hallucinations in DLB (Caminiti et al., 2019). Notably, male sex is considered the primary predictive factor in the transition from no cogni-

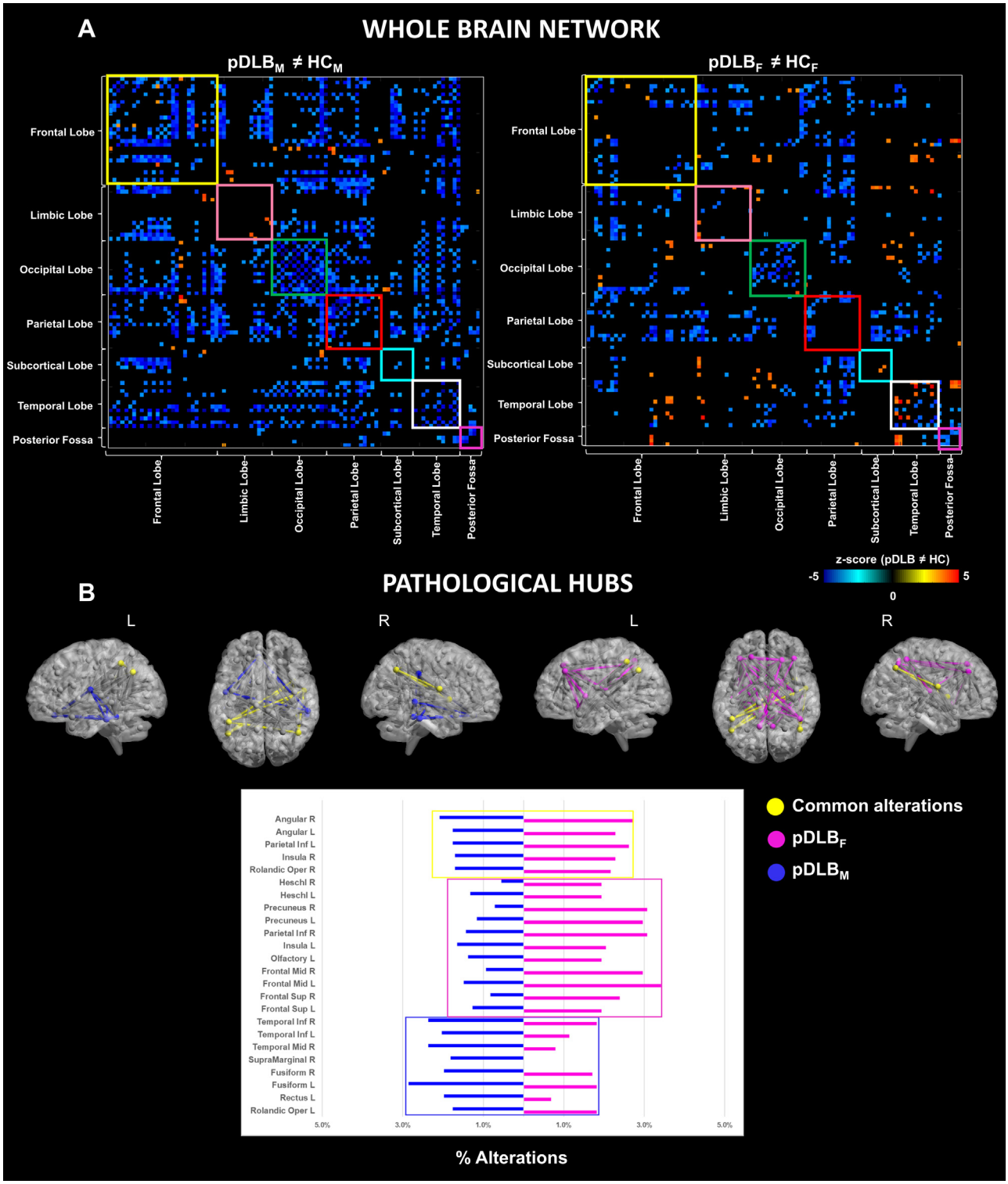

Fig. 2. Whole-brain network analysis. (A) The matrices represent the significant differences obtained comparing adjacency matrices ($p < 0.05$, uncorrected for multiple comparisons) between pDLB$_M$ versus age-sex matched control group and pDLB$_F$ versus age-sex matched control group in the whole brain network. The connectivity loss is shown in cyan-blu, the gained connectivity in yellow-red, and the unchanged connectivity in black. (B) 3D brain showing pathological hubs shared by the 2 groups (yellow) or specifically affected only in pDLB$_M$ (blue) or pDLB$_F$ (pink) groups. The pyramid plot shows the distribution of altered connectivity of the pathological hubs normalized to the total number of connectivity alterations in pDLB versus HC comparisons. Automated Anatomical Labeling (AAL) (Tzourio-Mazoyer et al., 2002) atlas' labels were grouped into 7 macro-regions for visualization porpouse: Frontal Lobe (precentral gyrus, superior frontal gyrus, middle frontal gyrus, inferior frontal gyrus, Rolandic operculum, supplementary motor area, olfactory lobe, rectus gyrus), limbic lobe (insula, anterior cingulate cortex, middle cingulate cortex, posterior cingulate cortex, hippocampus, parahippocampal gyrus, amygdala), occipital lobe (calcarine cortex, cuneus, lingual gyrus, superior occipital gyrus, middle occipital gyrus, inferior occipital gyrus), parietal lobe (precentral gyrus, superior parietal lobule, inferior parietal lobule, supramarginal gyrus, angular gyrus, precuneus, paracentral lobule), subcortical lobe (caudate, putamen, thalamus, pallidum), temporal lobe (fusiform gyrus, Heschl gyrus, superior temporal gyrus, superior temporal pole, middle temporal gyrus, middle temporal pole, inferior temporal gyrus), and posterior fossa (cerebellum crus, lobules and vermis). Abbreviations: F, Females; HC, Healthy Controls; L, left; R, right; M, males; pDLB, probable dementia with Lewy bodies. (For interpretation of the references to color in this figure legend, the reader is referred to the Web version of this article.)

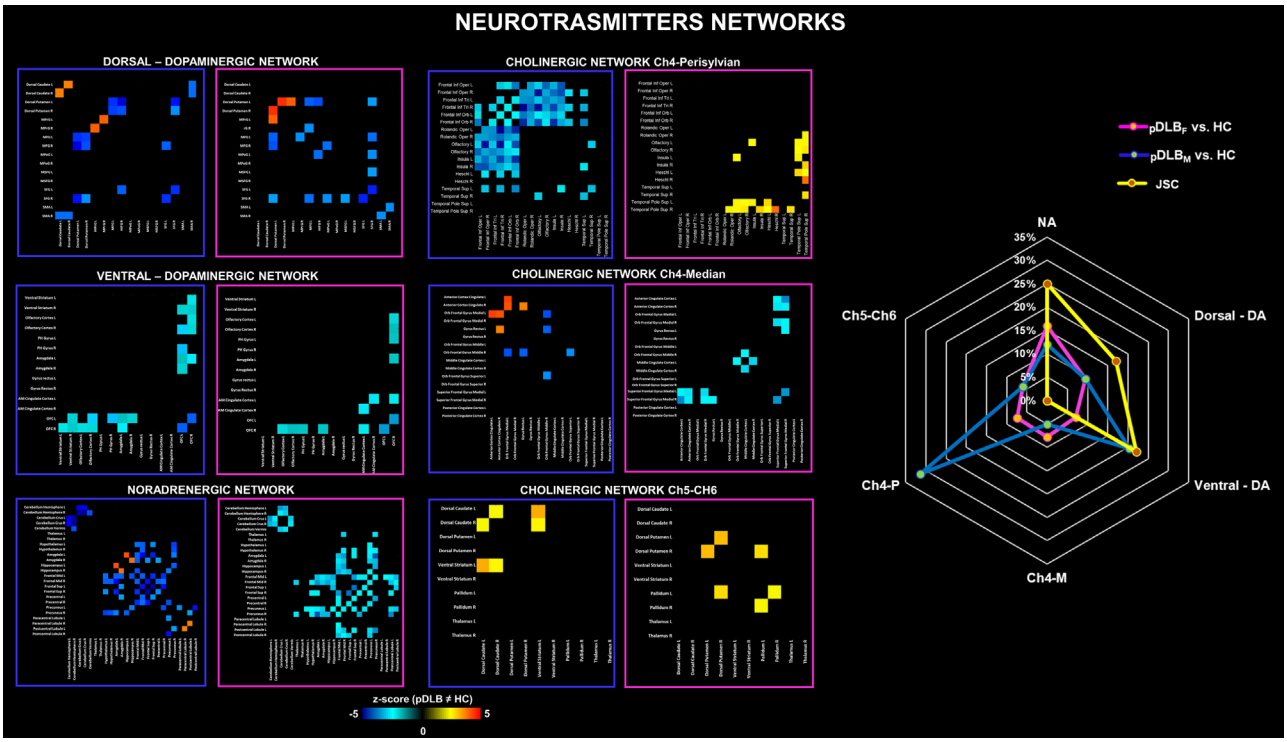

Fig. 3. Neurotransmitter networks analysis. The matrices represent the significant differences obtained comparing adjacency matrices ($p < 0.05$, uncorrected for multiple comparisons) between pDLB$_M$ versus age-sex matched control group (square blue) and pDLB$_F$ versus age-sex matched control group (square pink) in the different neurotransmitter networks. The connectivity loss is shown in cyan, the gained connectivity in yellow, and the unchanged connectivity in black. Radar plot showing the percentage of altered connections in pDLB$_F$ (pink line), pDLB$_M$ (blue line), and the common alterations JSC (yellow line) in the 2 clinical groups. Abbreviations: Ch, Cholinergic; Ch-M, Cholinergic-Median; Ch-P, Cholinergic-Perisylvian; DA, dopaminergic; F, females; HC, healthy controls; JSC, Jaccard Similarity Coefficient; M, males; NA, noradrenergic; pDLB, probable dementia with Lewy bodies. (For interpretation of the references to color in this figure legend, the reader is referred to the Web version of this article.)

tive impairment to mild cognitive impairment or dementia in patients with PD and men progress more rapidly than women (Cholerton et al., 2018). Moreover, a recent longitudinal PET study reported an annually increased tau accumulation in the lateral occipital cortices, inferior parietal cortex, and fusiform gyrus in patients with DLB. The longitudinal increase in tau accumulation observed in both the fusiform gyrus and occipital cortex correlated also with global cognitive decline measures (Chen et al., 2022). We also found more severe hypometabolism in the hippocampus in pDLB$_F$ than pDLB$_M$ (Fig. 1). A recent postmortem study showed more severe hypometabolism in the hippocampus in patients with both concomitant LB and AD pathology than with only LB (Lee et al., 2022). Co-occurrent AD pathology is more often observed in DLB females than males (Bayram et al., 2021; Coughlin et al., 2020). Sex was found to significantly impact on AD copathology, with women showing a higher expression (Bayram et al., 2022).

In the present study we also evaluated the linear relationship between hypometabolism and age in the males and females HC. We found in both males and females a medial frontal cortex hypometabolism associated with aging, that was more extended in males than females (see Supplementary Fig. 1). The present results confirm the previous evidence of a more extended frontal lobe vulnerability in males than females (Malpetti et al., 2017). The frontal lobe vulnerability related to aging was consistently reported in the literature (Kakimoto et al., 2016; Knopman et al., 2014; Tisserand & Jolles, 2003), and sex differences in age-related hypometabolism might reflect the faster age-related cognitive declines in males (Gur & Gur, 2022). In addition, in elderly males, declining levels of circulating testosterone are linked to changes in brain function and cognition (see [Giagulli et al., 2016] for review).

Previously published studies revealed whole-brain metabolic connectivity alterations in synucleinopathies (Caminiti et al., 2017; Sala et al., 2017). A widespread impairment of brain metabolic connectivity architecture was also found here in the pDLB cohort, with a more pronounced connectivity loss in the pDLB$_M$ than in the pDLB$_F$ group (Fig. 2B). Considering pDLB males and females separately, shared or specific metabolic connectivity alterations emerged in the present study. The shared connectivity alterations involved insular and parietal nodes disconnecting with both cortical and subcortical nodes. The pathological hubs localized in temporoparietal regions were in line with the typical DLB hypometabolic pattern (Caminiti et al., 2019). The insula emerged as an important pathological hub both in females and males showing disconnections from frontal and occipitoparietal regions. The insula is a complex structure multiconnected with several cortical regions. The insular lobe has the complex role of integrating information within and across cognitive, affective, visual, and sensorimotor tasks (Benarroch, 2019). Pathological studies found that this structure, in particular the anterior agranular insula, is an early site for pathological LB accumulations (Fathy et al., 2019). Consistently, neuroimaging studies detected hypoperfusion (Nagahama et al., 2010), dopamine deficit (Pilotto et al., 2019), decreased functional connectivity (Peraza et al., 2014), and lower fractional anisotropy value (Lee et al., 2010) in the insular cortex in DLB. Of note, together with the olfactory cortex, the insula showed increased connectivity with basal ganglia and limbic regions in pDLB$_F$. Increased connectivity is emerging as a fundamental response to the early phase of neurodegenerative processes (Hillary & Grafman, 2017). The insular hyperconnectivity found in females, is of particular interest, considering that the node emerged, instead, as a pathological hub for its prevalent losses in pDLB$_M$.

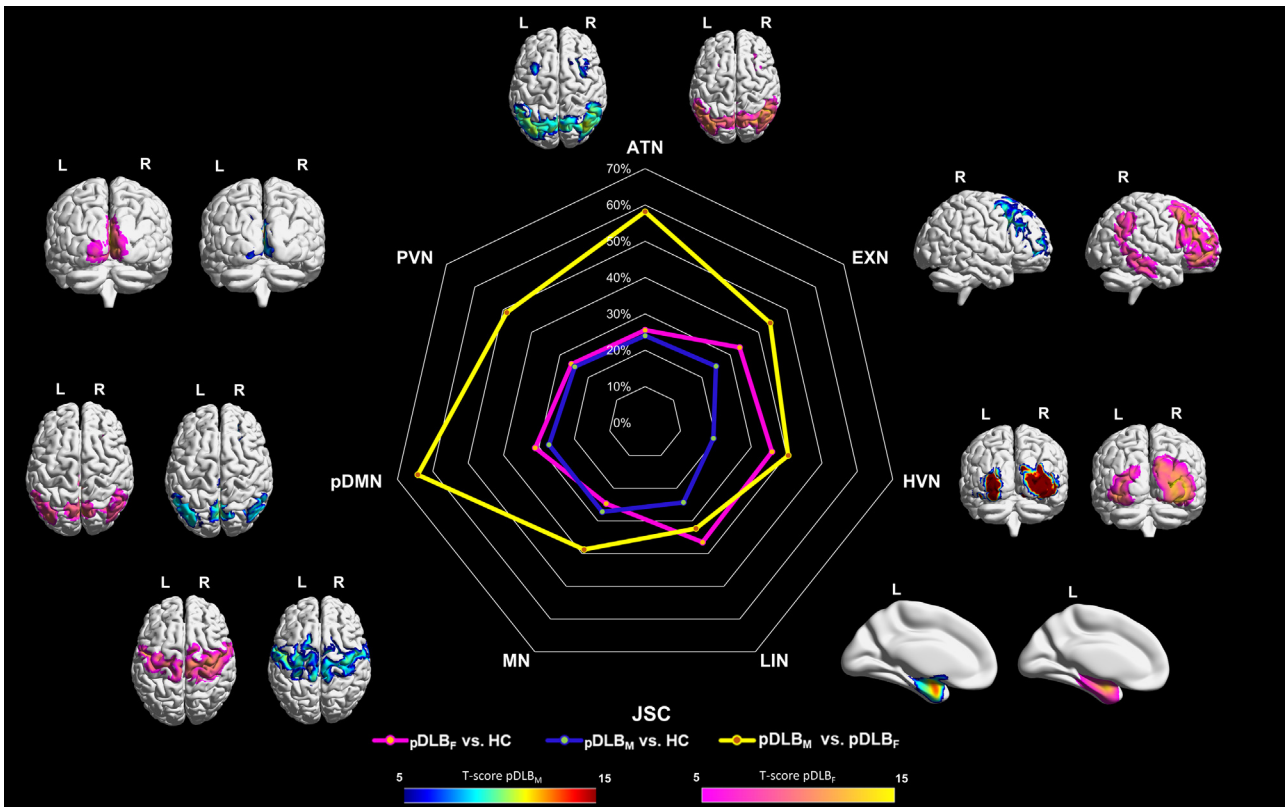

Fig. 4. Resting state network analysis. Resting state network connectivity in pDLB males and females' groups. Blue/red scale represents correlation strength (T-score) between network's seed and the rest of the brain in $pDLB_M$ ($p < 0.05$, Family-wise Error corrected, k = 100); Pink/yellow scale represents correlation strength (T-score) between network's seed and the rest of the brain in $pDLB_F$ ($p < 0.05$, Family-wise Error corrected, k = 100). Radar plot showing JSC obtained comparing pDLB groups with HC and males and females DLB groups. The pink line indicates overlap, measured by JSC, between $pDLB_F$ and HC RSNs, the blue line indicates overlap between $pDLB_M$ and HC RSNs and the yellow line indicates the overlap between $pDLB_F$ and $pDLB_M$ in RSNs. 3D renderings were obtained from BrainNet Viewer toolbox (Xia et al., 2013). Abbreviations: ATN, attention network; EXN, executive network; F, females; HC, healthy controls; HVN, higher visual network; JSC, Jaccard Similarity Coefficient; LIN, limbic network; M, males; MN, motor network; pDLB probable dementia with Lewy Bodies; PVN, primary visual network; RSNs, resting state networks. (For interpretation of the references to color in this figure legend, the reader is referred to the Web version of this article.)

DLB females and males also showed specific sex-related pathological hubs: for females, hubs were localized in the precuneus, frontal and parietal regions, whereas for males, hubs were found in the inferior temporal and fusiform gyri. The different locations of pathological hubs according to sex, here might indicate specific regional vulnerability not only driven by the LB pathology.

The brain multisystem connectivity impairment in DLB is paralleled by metabolic connectivity data targeting neurotransmission systems, such as the dopaminergic, noradrenergic, and cholinergic networks (Caminiti et al., 2017; Carli et al., 2020). Here, the analysis of the neurotransmitters' networks showed that the 2 pDLB groups shared the most important connectivity alterations in the dorsal and ventral dopaminergic networks as well as in noradrenergic pathways (Fig. 3). The *dopaminergic network* dysfunction was similar for the dorsal division in the groups but was slightly more affected in $pDLB_M$ for the ventral division. These results support the significant alteration of the dopaminergic networks in pDLB (Carli et al., 2020), independently of sex. Notably, we found more subcortical local alterations in men, involving the caudate and the ventral striatum compared to females whose alterations, instead, affected the subcortical-cortical connections. The *noradrenergic network* dysfunction is considered an early pathological event in the α-synuclein-spectrum and an extended reconfiguration of this network is already present in idiopathic RBD (Carli et al., 2020). Our data support that noradrenergic pathology deficiency is of great magnitude in synucleinopathies (Vermeiren & De Deyn, 2017) and can explain not only the autonomic and sleep disturbances but also cognitive performances (Gratwicke et al., 2015). In the current study, sex differences emerged in the connectivity of the *cholinergic networks*, with males showing more severe alterations with different connectivity patterns than females. The differences were strong in the Ch4-perisylvian division. Males showed the most important reduction in connectivity in this network affecting almost all nodes, females instead showed increased connectivity to the insula, frontal, temporal, and olfactory cortices. Comparable sex differences emerged also in the Ch4-Median and Ch5-Ch6 divisions. According to the "compensatory hypothesis", increased cholinergic activity in cortical circuits may compensate for executive dysfunctions associated with striatal dopaminergic declines in the early stages of LB disorders (Bohnen et al., 2018). In this perspective, the here reported increased cholinergic connectivity in $pDLB_F$ could represent an attempt to compensate for a system that is instead already disrupted in $pDLB_M$. However, a form of maladaptive functional reorganization resulting from the brain's failure to cope with the damage cannot be excluded (Hillary & Grafman, 2017). For instance, the proper one-to-one connection in healthy brains can be replaced by a widespread dysfunctional connectivity pattern represented by increases between several regions. Moreover, it is worth noting that hyperconnectivity may also have a detrimental role in driving the spreading of neurodegeneration (Hillary & Grafman, 2017). However, separating beneficial from maladaptive processes remains challenging in need of correlations with clinical data (Schoonheim, 2017). The involvement of the Ch5-Ch6 pathway and the loss of Ch4 projections from the

nucleus basalis of Meynert to cortical structures is in line with previous metabolic connectivity (Caminiti et al., 2017) and tracer-specific cholinergic neurotransmission studies (Kanel et al., 2021). Cholinergic neurotransmission has a crucial role in cognitive function, supported also by the association between cholinergic depletion and cognitive decline in LB disorders (Bohnen et al., 2018). However, no previous *in vivo* imaging studies focused on sex differences in the cholinergic system in DLB. Research in healthy animals revealed no marked difference in the general morphology of the brain cholinergic system, but subtle functional sex differences. In humans, sex differences in the nucleus basalis of Meynert exist (Giacobini & Pepeu, 2018). Many estradiol receptors are present in the basal forebrain cholinergic neurons and estradiol appears to modulate the cholinergic system through trophic effects (Newhouse & Dumas, 2015). Moreover, lifetime estrogen exposure might protect against the AD dementia risk that is associated with reduced estrogen levels (Zhu et al., 2021). Comparably, in PD, a possible neuroprotective effect of estradiol on this neurotransmission system is suggested, with the male sex as the main risk factor of progressing to dementia (Cholerton et al., 2018). Further studies using specific radioligands for the vesicular acetylcholine transporter, such as [18F]-fluoroethoxybenzovesamicol, might highlight the way DLB pathology differently affects the cholinergic system and the related cognitive dysfunction in males and females.

Previous metabolic connectivity evidence showed a severe involvement of RSNs, such as the posterior cortical, the limbic, and the attention networks, whose disruption is strongly related to the DLB clinical symptoms (Sala et al., 2019). Considering females and males separately, the *RSNs* showed similar reconfigurations in the 2 groups, with the confirmation of the main involvement of pDMN, attentive, and motor networks (Fig. 4). A previous study investigating RSNs' integrity and their interactions with DLB core symptoms reported significant alterations of pDMN, as well as the limbic and attention networks in a DLB cohort (Sala et al., 2019). Regarding sex-specific alterations, the limbic network was more dysfunctional in $pDLB_M$ than $pDLB_F$. The amygdala is the seed driving the limbic network's construction. According to the recent "brain-first" hypothesis of α-synuclein spreading, the amygdala seems to be the most likely site of origin of LB pathology (Horsager et al., 2020). The initial prevalent involvement of the amygdala was associated with an increased likelihood of PD evolving toward DLB (Blesa et al., 2022). Recently, the amygdala volume has been reported to be associated with the trajectories of hallucinations, but not with other neuropsychiatric symptoms as happening in AD (Jaramillo-Jimenez et al., 2021), and an increased burden of LB in the amygdala was present in DLB patients with visual hallucinations (O'brien et al., 2020).

In conclusion, we identified a common metabolic connectivity substrate in men and women with a clinical diagnosis of pDLB. The shared connectivity alterations are also associated with the posterior cortical vulnerability which univocally characterizes the DLB condition, independently by sex effects. However, $pDLB_M$ showed more severe brain hypometabolism and long-distance connectivity alterations in the prototypical damaged DLB regions, which can explain a more clear-cut symptom-related diagnosis in males than females

Given the recent evidence of AD copathology as a possible driver of sex differences, further prospective studies combining brain metabolism and pathological measures, such as the CSF measures, are necessary . The lack of a comparable and full neuropsychological assessment in the present cohort represents a limitation preventing the evaluation of sex effects on the cognitive-neuroimaging correlations, a crucial point to be addressed by future studies.

The cholinergic denervation in the $pDLB_F$ group involving limbic predominant structures seems to be less affected than $pDLB_M$, in need of further investigation along the clinical/cognitive sex differences.

CRediT authorship contribution statement

Silvia Paola Caminiti: drafting/revision of the manuscript for content, including medical writing for content; study concept or design; analysis or interpretation of data. *Cecilia Boccalini*: drafting/revision of the manuscript for content, including medical writing for content; major role in the acquisition of data. *Nicolas Nicastro*: drafting/revision of the manuscript for content, including medical writing for content; major role in the acquisition of data. *Valentina Garibotto*: drafting/revision of the manuscript for content, including medical writing for content; major role in the acquisition of data. Daniela Perani: drafting/revision of the manuscript for content, including medical writing for content; study concept or design.

Disclosure statement

The author(s) declared no potential conflicts of interest with respect to the research, authorship, and /or publication of this article. The author(s) received no financial support for the research, authorship, and/or publication of this article.

Submission declaration and verification

The present work has not been published previously, it is not under consideration for publication elsewhere, its publication is approved by all authors and tacitly or explicitly by the responsible authorities where the work was carried out, and, if accepted, it will not be published elsewhere in the same form, in English or in any other language, including electronically without the written consent of the copyright-holder.

Data availability

Data supporting the present findings are available upon reasonable request.

Supplementary materials

Supplementary material associated with this article can be found, in the online version, at doi:10.1016/j.neurobiolaging.2023.02.004.

References

A Giagulli, V., Guastamacchia, E., Licchelli, B., Triggiani, V., 2016. Serum testosterone and cognitive function in ageing male: updating the evidence. Recent Pat. Endocr. Metab. Immune Drug Discov. 10, 22–30.

Abdelnour, C., Ferreira, D., van de Beek, M., Cedres, N., Oppedal, K., Cavallin, L., Blanc, F., Bousiges, O., Wahlund, L.-O., Pilotto, A., 2022. Parsing heterogeneity within dementia with Lewy bodies using clustering of biological, clinical, and demographic data. Alzheimers. Res. Ther. 14, 1–13.

Ballmaier, M., O'Brien, J.T., Burton, E.J., Thompson, P.M., Rex, D.E., Narr, K.L., McKeith, I.G., DeLuca, H., Toga, A.W., 2004. Comparing gray matter loss profiles between dementia with Lewy bodies and Alzheimer's disease using cortical pattern matching: diagnosis and gender effects. Neuroimage 23, 325–335. doi:10.1016/j.neuroimage.2004.04.026.

Barnes, L.L., Lamar, M., Schneider, J.A., 2019. Sex differences in mixed neuropathologies in community-dwelling older adults. Brain Res 1719, 11–16.

Bayram, E., Coughlin, D.G., Banks, S.J., Litvan, I., 2021. Sex differences for phenotype in pathologically defined dementia with Lewy bodies. J. Neurol. Neurosurg. Psychiatry 92, 745–750.

Bayram, E., Coughlin, D.G., Litvan, I., 2022. Sex differences for clinical correlates of Alzheimer's pathology in people with Lewy body pathology. Mov. Disord. 37, 1505–1515.

Benarroch, E.E., 2019. Insular cortex: functional complexity and clinical correlations. Neurology 93, 932–938.
Bennett, C.M., Wolford, G.L., Miller, M.B., 2009. The principled control of false positives in neuroimaging. Soc. Cogn. Affect. Neurosci. 4, 417–422.
Blesa, J., Foffani, G., Dehay, B., Bezard, E., Obeso, J.A., 2022. Motor and non-motor circuit disturbances in early Parkinson disease: which happens first? Nat. Rev. Neurosci. 23, 115–128.
Boccalini, C., Carli, G., Pilotto, A., Padovani, A., Perani, D., 2022. Gender differences in dopaminergic system dysfunction in de novo Parkinson's disease clinical subtypes. Neurobiol. Dis. 167, 105668.
Boccalini, C., Carli, G., Pilotto, A., Padovani, A., Perani, D., 2020. Gender-related vulnerability of dopaminergic neural networks in Parkinson's disease. Brain Connect 11, 1–28. doi:10.1089/brain.2020.0781.
Bohnen, N.I., Grothe, M.J., Ray, N.J., Müller, M.L.T.M., Teipel, S.J., 2018. Recent advances in cholinergic imaging and cognitive decline—revisiting the cholinergic hypothesis of dementia. Curr. Geriatr. Reports 7, 1–11. doi:10.1007/s13670-018-0234-4.
Caminiti, S., Tettamanti, M., Sala, A., Presotto, L., Iannaccone, S., Cappa, S.F., Magnani, G., Perani, D., 2017. Metabolic connectomics targeting brain pathology in dementia with Lewy bodies. J. Cereb. Blood Flow Metab. 37, 1311–1325. doi:10.1177/0271678X16654497.
Caminiti, S.P., Carli, G., 2023. Molecular Imaging Evidence in Favor or Against PDD and DLB Overlap, In: Neuroimaging in Parkinson s Disease and Related Disorders. Academic Press, pp. 275–295.
Caminiti, Silvia Paola, Sala, A., Iaccarino, L., Beretta, L., Pilotto, A., Gianolli, L., Iannaccone, S., Magnani, G., Padovani, A., Ferini-Strambi, L., Perani, D., 2019. Brain glucose metabolism in Lewy body dementia: implications for diagnostic criteria. Alzheimer's Res. Ther. 11, 20. doi:10.1186/s13195-019-0473-4.
Caminiti, S.P., Sala, A., Presotto, L., Chincarini, A., Sestini, S., Perani, D., Schillaci, O., Berti, V., Calcagni, M.L., Cistaro, A., 2021. Validation of FDG-PET datasets of normal controls for the extraction of SPM-based brain metabolism maps. Eur. J. Nucl. Med. Mol. Imaging 48 (8), 2486–2499.
Caminiti, S.P., Tettamanti, M., Sala, A., Presotto, L., Iannaccone, S., Cappa, S.F., Magnani, G., Perani, D., 2017. Metabolic connectomics targeting brain pathology in dementia with Lewy bodies. J. Cereb. Blood Flow Metab. 37, 1311–1325. doi:10.1177/0271678X16654497.
Carli, G., Caminiti, S.P., Sala, A., Galbiati, A., Pilotto, A., Ferini-Strambi, L., Padovani, A., Perani, D., 2020. Impaired metabolic brain networks associated with neurotransmission systems in the α-synuclein spectrum. Parkinsonism Relat Disord. 81, 113–122. doi:10.1016/j.parkreldis.2020.10.036.
Carli, G., Tondo, G., Boccalini, C., Perani, D., 2021. Brain Molecular Connectivity in Neurodegenerative Conditions. Brain Sci 11, 433.
Caslake, R., Taylor, K., Scott, N., Gordon, J., Harris, C., Wilde, K., Murray, A., Counsell, C., 2013. Age-, gender-, and socioeconomic status-specific incidence of Parkinson's disease and Parkinsonism in North East Scotland: the PINE study. Parkinsonism Relat. Disord. 19, 515–521.
Chen, Q., Przybelski, S.A., Senjem, M.L., Schwarz, C.G., Lesnick, T.G., Botha, H., Knopman, D.S., Graff-Radford, J., Savica, R., Jones, D.T., 2022. Longitudinal tau positron emission tomography in dementia with Lewy bodies. Mov. Disord. 37, 1256–1264.
Cholerton, B., Johnson, C.O., Fish, B., Quinn, J.F., Chung, K.A., Peterson-Hiller, A.L., Rosenthal, L.S., Dawson, T.M., Albert, M.S., Hu, S.-C., 2018. Sex differences in progression to mild cognitive impairment and dementia in Parkinson's disease. Parkinsonism Relat. Disord. 50, 29–36.
Coughlin, D.G., Hurtig, H.I., Irwin, D.J., 2020. Pathological influences on clinical heterogeneity in Lewy body diseases. Mov. Disord. 35, 5–19. doi:10.1002/mds.27867.
Della Rosa, P.A., Cerami, C., Gallivanone, F., Prestia, A., Caroli, A., Castiglioni, I., Gilardi, M.C., Frisoni, G., Friston, K., Ashburner, J., 2014. A standardized [18 F]-FDG-PET template for spatial normalization in statistical parametric mapping of dementia. Neuroinformatics 12, 575–593.
Dugger, B.N., Boeve, B.F., Murray, M.E., Parisi, J.E., Fujishiro, H., Dickson, D.W., Ferman, T.J., 2012. Rapid eye movement sleep behavior disorder and subtypes in autopsy-confirmed dementia with Lewy bodies. Mov. Disord. 27, 72–78.
Eickhoff, S.B., Stephan, K.E., Mohlberg, H., Grefkes, C., Fink, G.R., Amunts, K., Zilles, K., 2005. A new SPM toolbox for combining probabilistic cytoarchitectonic maps and functional imaging data. Neuroimage 25, 1325–1335. doi:10.1016/j.neuroimage.2004.12.034.
Fathy, Y.Y., Jonker, A.J., Oudejans, E., de Jong, F.J.J., van Dam, A., Rozemuller, A.J.M., van de Berg, W.D.J., 2019. Differential insular cortex subregional vulnerability to α-synuclein pathology in Parkinson's disease and dementia with Lewy bodies. Neuropathol. Appl. Neurobiol. 45, 262–277.
Ferretti, M.T., Iulita, M.F., Cavedo, E., Chiesa, P.A., Schumacher Dimech, A., Santuccione Chadha, A., Baracchi, F., Girouard, H., Misoch, S., Giacobini, E., 2018. Sex differences in Alzheimer disease—the gateway to precision medicine. Nat. Rev. Neurol. 14, 457–469.
Francis, P.T., Perry, E.K., 2007. Cholinergic and other neurotransmitter mechanisms in Parkinson's disease, Parkinson's disease dementia, and dementia with Lewy bodies. Mov. Disord. Off. J. Mov. Disord. Soc. 22, S351–S357.
Giacobini, E., Pepeu, G., 2018. Sex and gender differences in the brain cholinergic system and in the response to therapy of Alzheimer disease with cholinesterase inhibitors. Curr. Alzheimer Res. 15, 1077–1084.
Gratwicke, J., Jahanshahi, M., Foltynie, T., 2015. Parkinson's disease dementia: a neural networks perspective. Brain 138, 1454–1476.
Gur, R.C., Richard, J., Calkins, M.E., Chiavacci, R., Hansen, J.A., Bilker, W.B., Loughead, J., Connolly, J.J., Qiu, H., Mentch, F.D., 2012. Age group and sex differences in performance on a computerized neurocognitive battery in children age 8–21. Neuropsychology 26, 251.
Gur, R.E., Gur, R.C., 2022. Gender differences in aging: cognition, emotions, and neuroimaging studies. Dialogues Clin. Neurosci. 4, 197–210.
Habich, A., Wahlund, L.-O., Westman, E., Dierks, T., Ferreira, D., 2022. (Dis-) connected dots in dementia with Lewy bodies-a systematic review of connectivity studies. Mov. Disord. 38, 4–15.
Hillary, F.G., Grafman, J.H., 2017. Injured brains and adaptive networks: the benefits and costs of hyperconnectivity. Trends Cogn. Sci. 21, 385–401.
Horsager, J., Andersen, K.B., Knudsen, K., Skjærbæk, C., Fedorova, T.D., Okkels, N., Schaeffer, E., Bonkat, S.K., Geday, J., Otto, M., 2020. Brain-first versus body–first Parkinson's disease: a multimodal imaging case-control study. Brain 143, 3077–3088.
Horwitz, B., Duara, R., Rapoport, S.I., 1984. Intercorrelations of glucose metabolic rates between brain regions: application to healthy males in a state of reduced sensory input. J. Cereb. Blood Flow Metab. 4, 484–499.
Ingalhalikar, M., Smith, A., Parker, D., Satterthwaite, T.D., Elliott, M.A., Ruparel, K., Hakonarson, H., Gur, R.E., Gur, R.C., Verma, R., 2014. Sex differences in the structural connectome of the human brain. Proc. Natl. Acad. Sci 111, 823–828.
Jaramillo-Jimenez, A., Giil, L.M., Tovar-Rios, D.A., Borda, M.G., Ferreira, D., Brønnick, K., Oppedal, K., Aarsland, D., 2021. Association between amygdala volume and trajectories of neuropsychiatric symptoms in Alzheimer's disease and dementia with Lewy bodies. Front. Neurol. 12, 1–13. doi:10.3389/fneur.2021.679984.
Jones, D.T., MacHulda, M.M., Vemuri, P., McDade, E.M., Zeng, G., Senjem, M.L., Gunter, J.L., Przybelski, S.A., Avula, R.T., Knopman, D.S., Boeve, B.F., Petersen, R.C., Jack, C.R., 2011. Age-related changes in the default mode network are more advanced in Alzheimer disease. Neurology 77, 1524–1531. doi:10.1212/WNL.0b013e318233b33d.
Jovicich, J., Minati, L., Marizzoni, M., Marchitelli, R., Sala-Llonch, R., Bartrés-Faz, D., Arnold, J., Benninghoff, J., Fiedler, U., Roccatagliata, L., Picco, A., Nobili, F., Blin, O., Bombois, S., Lopes, R., Bordet, R., Sein, J., Ranjeva, J.P., Didic, M., Gros-Dagnac, H., Payoux, P., Zoccatelli, G., Alessandrini, F., Beltramello, A., Bargalló, N., Ferretti, A., Caulo, M., Aiello, M., Cavaliere, C., Soricelli, A., Parnetti, L., Tarducci, R., Floridi, P., Tsolaki, M., Constantinidis, M., Drevelegas, A., Rossini, P.M., Marra, C., Schönknecht, P., Hensch, T., Hoffmann, K.T., Kuijer, J.P., Visser, P.J., Barkhof, F., Frisoni, G.B., 2016. Longitudinal reproducibility of default-mode network connectivity in healthy elderly participants: a multicentric resting-state fMRI study. Neuroimage 124, 442–454. doi:10.1016/j.neuroimage.2015.07.010.
Kakimoto, A., Ito, S., Okada, H., Nishizawa, S., Minoshima, S., Ouchi, Y., 2016. Age-related sex-specific changes in brain metabolism and morphology. J. Nucl. Med. 57, 221–225.
Kanel, P., Bedard, M.A., Aghourian, M., Rosa-Neto, P., Soucy, J.P., Albin, R.L., Bohnen, N.I., 2021. Molecular imaging of the cholinergic system in Alzheimer and Lewy body dementias: expanding views. Curr. Neurol. Neurosci. Rep. 21, 1–9. doi:10.1007/s11910-021-01140-z.
Karahanoğlu, F.I., Van De Ville, D., 2015. Transient brain activity disentangles fMRI resting-state dynamics in terms of spatially and temporally overlapping networks. Nat. Commun. 6, 7751. doi:10.1038/ncomms8751.
Kasanuki, K., Iseki, E., Fujishiro, H., Yamamoto, R., Higashi, S., Minegishi, M., Togo, T., Katsuse, O., Uchikado, H., Furukawa, Y., 2012. Neuropathological investigation of the hypometabolic regions on positron emission tomography with [18F] fluorodeoxyglucose in patients with dementia with Lewy bodies. J. Neurol. Sci. 314, 111–119.
Knopman, D.S., Jack Jr, C.R., Wiste, H.J., Lundt, E.S., Weigand, S.D., Vemuri, P., Lowe, V.J., Kantarci, K., Gunter, J.L., Senjem, M.L., 2014. 18F-fluorodeoxyglucose positron emission tomography, aging, and apolipoprotein E genotype in cognitively normal persons. Neurobiol. Aging 35, 2096–2106.
Lee, D.S., Kang, H., Kim, H., Park, H., Oh, J.S., Lee, J.S., Lee, M.C., 2008. Metabolic connectivity by interregional correlation analysis using statistical parametric mapping (SPM) and FDG brain PET; methodological development and patterns of metabolic connectivity in adults. Eur. J. Nucl. Med. Mol. Imaging 35, 1681–1691.
Lee, J.E., Park, H.-J., Park, B., Song, S.K., Sohn, Y.H., Lee, J.D., Lee, P.H., 2010. A comparative analysis of cognitive profiles and white-matter alterations using voxel-based diffusion tensor imaging between patients with Parkinson's disease dementia and dementia with Lewy bodies. J. Neurol. Neurosurg. Psychiatry 81, 320–326.
Lee, Y.gun, Jeon, S., Park, M., Kang, S.W., Yoon, S.H., Baik, K., Lee, P.H., Sohn, Y.H., Ye, B.S., 2022. Effects of Alzheimer and Lewy Body Disease Pathologies on Brain Metabolism. Ann. Neurol. 91, 853–863. doi:10.1002/ana.26355.
Malpetti, M., Ballarini, T., Presotto, L., Garibotto, V., Tettamanti, M., Perani, D.(NEST-DD) database, 2017. Gender differences in healthy aging and Alzheimer's Dementia: a 18F-FDG-PET study of brain and cognitive reserve. Hum. Brain Mapp. 38, 4212–4227.
McKeith, I.G., Boeve, B.F., Dickson, D.W., Halliday, G., Taylor, J.-P., Weintraub, D., Aarsland, D., Galvin, J., Attems, J., Ballard, C.G., 2017. Diagnosis and management of dementia with Lewy bodies: fourth consensus report of the DLB Consortium. Neurology 89, 88–100.
Mouton, A., Blanc, F., Gros, A., Manera, V., Fabre, R., Sauleau, E., Gomez-Luporsi, I., Tifratene, K., Friedman, L., Thümmler, S., 2018. Sex ratio in dementia with Lewy bodies balanced between Alzheimer's disease and Parkinson's disease dementia: a cross-sectional study. Alzheimers. Res. Ther. 10, 1–10.

Nagahama, Y., Okina, T., Suzuki, N., Matsuda, M., 2010. Neural correlates of psychotic symptoms in dementia with Lewy bodies. Brain 133, 557–567.

Nelson, P.T., Schmitt, F.A., Jicha, G.A., Kryscio, R.J., Abner, E.L., Smith, C.D., Van Eldik, L.J., Markesbery, W.R., 2010. Association between male gender and cortical Lewy body pathology in large autopsy series. J. Neurol. 257, 1875–1881.

Newhouse, P., Dumas, J., 2015. Hormones and behavior estrogen – cholinergic interactions : implications for cognitive aging. Horm. Behav. 74, 173–185. doi:10.1016/j.yhbeh.2015.06.022.

O'brien, J., Taylor, J.P., Ballard, C., Barker, R.A., Bradley, C., Burns, A., Collerton, D., Dave, S., Dudley, R., Francis, P., Gibbons, A., Harris, K., Lawrence, V., Leroi, I., Mckeith, I., Michaelides, M., Naik, C., O'callaghan, C., Olsen, K., Onofrj, M., Pinto, R., Russell, G., Swann, P., Thomas, A., Urwyler, P., Weil, R.S., Ffytche, D., 2020. Visual hallucinations in neurological and ophthalmological disease: pathophysiology and management. J. Neurol. Neurosurg. Psychiatry 91, 512–519. doi:10.1136/jnnp-2019-322702.

Perani, D., Della Rosa, P.A., Cerami, C., Gallivanone, F., Fallanca, F., Vanoli, E.G., Panzacchi, A., Nobili, F.M., Pappatà, S., Marcone, A., Garibotto, V., Castiglioni, I., Magnani, G., Cappa, S.F., Gianolli, L., Drzezga, A., Perneczky, R., Didic, M., Guedj, E., Van Berckel, B.N., Ossenkoppele, R., Morbelli, S., Frisoni, G.B., Caroli, A., 2014. Validation of an optimized SPM procedure for FDG-PET in dementia diagnosis in a clinical setting. NeuroImage Clin 6, 445–454. doi:10.1016/j.nicl.2014.10.009.

Perani, D., Sala, A., Caminiti, S.P., Presotto, L., Pilotto, A., Liguori, C., Chiaravalloti, A., Garibotto, V., Frisoni, G.B., D'Amelio, M., 2021. In vivo human molecular neuroimaging of dopaminergic vulnerability along the Alzheimer's disease phases. Alzheimers Res Ther 13, 187.

Peraza, L.R., Kaiser, M., Firbank, M., Graziadio, S., Bonanni, L., Onofrj, M., Colloby, S.J., Blamire, A., O'Brien, J., Taylor, J.-P., 2014. fMRI resting state networks and their association with cognitive fluctuations in dementia with Lewy bodies. NeuroImage Clin. 4, 558–565.

Pfeiffer, R.F., 2016. Non-motor symptoms in Parkinson's disease. Parkinsonism Relat. Disord. 22, S119–S122.

Pilotto, A., Di Cola, F.S., Premi, E., Grasso, R., Turrone, R., Gipponi, S., Scalvini, A., Cottini, E., Paghera, B., Garibotto, V., 2019. Extrastriatal dopaminergic and serotonergic pathways in Parkinson's disease and in dementia with Lewy bodies: a 123 I-FP-CIT SPECT study. Eur. J. Nucl. Med. Mol. Imaging 46, 1642–1651.

Podcasy, J.L., Epperson, C.N., 2022. Considering sex and gender in Alzheimer disease and other dementias. Dialogues Clin. Neurosci 18, 437–446.

Presotto, L., Ballarini, T., Caminiti, S.P., Bettinardi, V., Gianolli, L., Perani, D., 2017. Validation of 18F–FDG-PET single-subject optimized SPM procedure with different PET scanners. Neuroinformatics 15, 151–163. doi:10.1007/s12021-016-9322-9.

Ruigrok, A.N.V, Salimi-Khorshidi, G., Lai, M.-C., Baron-Cohen, S., Lombardo, M.V, Tait, R.J., Suckling, J., 2014. A meta-analysis of sex differences in human brain structure. Neurosci. Biobehav. Rev. 39, 34–50.

Sala, A., Caminiti, S.P., Iaccarino, L., Beretta, L., Iannaccone, S., Magnani, G., Padovani, A., Ferini-Strambi, L., Perani, D., 2019. Vulnerability of multiple large-scale brain networks in dementia with Lewy bodies. Hum. Brain Mapp. 40, 4537–4550. doi:10.1002/hbm.24719.

Sala, A., Caminiti, S.P., Presotto, L., Premi, E., Pilotto, A., Turrone, R., Cosseddu, M., Alberici, A., Paghera, B., Borroni, B., Padovani, A., Perani, D., 2017. Altered brain metabolic connectivity at multiscale level in early Parkinson's disease. Sci. Rep. 7, 4256. doi:10.1038/s41598-017-04102-z.

Sallet, J., Mars, R.B., Noonan, M.P., Neubert, F.-X., Jbabdi, S., O'Reilly, J.X., Filippini, N., Thomas, A.G., Rushworth, M.F., 2013. The organization of dorsal frontal cortex in humans and macaques. J. Neurosci. 33, 12255–12274. doi:10.1523/JNEUROSCI.5108-12.2013.

Schoonheim, M.M., 2017. Functional reorganization is a maladaptive response to injury - commentary. Mult. Scler. 23, 194–196. doi:10.1177/1352458516677593.

Seeley, W.W., Menon, V., Schatzberg, a.F., Keller, J., Glover, G.H., Kenna, H., Reiss, a.L., Greicius, M.D., 2007. Dissociable intrinsic connectivity networks for salience processing and executive control. J. Neurosci. 27, 2349–2356. doi:10.1523/JNEUROSCI.5587-06.2007.

Shirer, W.R., Ryali, S., Rykhlevskaia, E., Menon, V., Greicius, M.D., 2012. Decoding subject-driven cognitive states with whole-brain connectivity patterns. Cereb. Cortex 22, 158–165. doi:10.1093/cercor/bhr099.

Tisserand, D.J., Jolles, J., 2003. On the involvement of prefrontal networks in cognitive ageing. Cortex 39, 1107–1128.

Tomasi, D., Volkow, N.D., 2011. Association between functional connectivity hubs and brain networks. Cereb. Cortex 21, 2003–2013. doi:10.1093/cercor/bhq268.

Tzourio-Mazoyer, N., Landeau, B., Papathanassiou, D., Crivello, F., Etard, O., Delcroix, N., Mazoyer, B., Joliot, M., 2002. Automated anatomical labeling of activations in SPM using a macroscopic anatomical parcellation of the MNI MRI single-subject brain. Neuroimage 15, 273–289. doi:10.1006/nimg.2001.0978.

van de Beek, M., Babapour Mofrad, R., van Steenoven, I., Vanderstichele, H., Scheltens, P., Teunissen, C.E., Lemstra, A.W., van der Flier, W.M., 2020. Sex-specific associations with cerebrospinal fluid biomarkers in dementia with Lewy bodies. Alzheimers. Res. Ther. 12, 1–8.

van Den Heuvel, M.P., Pol, H.E.H., 2010. Exploring the brain network: a review on resting-state fMRI functional connectivity. Eur. Neuropsychopharmacol. 20, 519–534.

Vermeiren, Y., De Deyn, P.P., 2017. Targeting the norepinephrinergic system in Parkinson's disease and related disorders: the locus coeruleus story. Neurochem. Int. 102, 22–32.

Xia, M., Wang, J., He, Y., 2013. BrainNet Viewer: a network visualization tool for human brain connectomics. PLoS One 8, e68910. doi:10.1371/journal.pone.0068910.

Zhu, D., Montagne, A., Zhao, Z., 2021. Alzheimer ' s pathogenic mechanisms and underlying sex difference. Cell. Mol. Life Sci. 78, 4907–4920. doi:10.1007/s00018-021-03830-w.